

NEUTRON DECAY OF CHARGE EXCHANGE GIANT RESONANCES IN
 $^{117,120}\text{Sn}(^3\text{He},t)$ AT $E(^3\text{He}) = 200$ MeV AND $\Theta_t = 0^\circ$

J. Jänecke, F. D. Becchetti, D. Roberts
University of Michigan, Ann Arbor, Michigan 48109

A. van den Berg and S.Y. van der Werf
Kernfysisch Versneller Instituut, Groningen, The Netherlands

G. P. A. Berg, J. Lisantti, R. Sawafta, and E. J. Stephenson
Indiana University Cyclotron Facility, Bloomington, Indiana 47480

M. N. Harakeh
Vrije Universiteit, Amsterdam, The Netherlands

A. Nadasen
Michigan State University, East Lansing, Michigan 48824

Much attention has been given in recent years to the investigation of spinflip (Gamow-Teller) resonances by means of the (p,n) charge-exchange reaction (e.g. Ref. 1). The present work combines the study of non-spinflip and spinflip resonances, including isobaric analog states (IAS), Gamow-Teller resonances (GT), and the $T_{<}$ component of the giant dipole resonance. It has been established previously² that the ($^3\text{He},t$) charge-exchange reaction at $E(^3\text{He}) = 200$ MeV (65 MeV/u) leads to a ratio of non-spinflip to spinflip matrix elements on the order of unity. Here, the K600 spectrometer was used to study the ($^3\text{He},t$) reaction on numerous targets from ^{12}C to ^{232}Th and ^{238}U at and near $\theta_t = 0^\circ$. The bombarding energy of 200 MeV ensures good momentum matching even for transitions to highly excited resonances. It is also high enough to push the maximum of the breakup/pickup continuum (at about 1/3 of the bombarding energy) to sufficiently high excitation energies that it doesn't obscure the giant resonances. An angular distribution for the transition to the IAS in ^{120}Sb measured from 0° to 16° was found to display very pronounced oscillatory structures with a sharp maximum at 0° and the first deep minimum at 3° in excellent agreement with microscopic calculations. This sharp forward maximum provides a characteristic signature for $L=0$ transitions.

The recent work represents another important extension of the previous work by including the detection of decay neutrons and γ rays following neutron emission. Measuring neutron decay from giant resonances in coincidence with tritons from the charge-exchange reactions is interesting in its own right. It also suppresses the nuclear continuum further and thus provides another signature for the detection of $L=0$ and $L=1$ giant resonances.

In the present experiment the tritons from the ($^3\text{He},t$) reaction were momentum analyzed with the K600 magnetic spectrometer at 0° . The $^3\text{He}^{++}$ beam of 5 nA with its much lower magnetic rigidity also entered the spectrograph but was stopped in an electrically insulated beam stop inside the first dipole magnet. This stop on the low momentum side reduced the solid angle by about 20%. Background in the focal plane detector originating from the beam stop was very weak.

Neutrons and γ rays produced in the ^{117}Sn and ^{120}Sn targets of 10 mg/cm^2 thickness were detected in small neutron detectors ($1.5'' \times 1.5''$; NE230, fully deuterated scintillation liquid C_6D_6) mounted inside the scattering chamber at $\Theta_n = 150^\circ$ at a distance of 6 cm from the target. Special precautions were taken to facilitate vacuum operation of scintillator, photomultiplier tube, and base. A Pb absorber of 4 mm thickness was mounted in front of the detector to reduce the high flux of low energy γ rays from the target. The count rate above threshold was about 11000 events/sec. The detector was calibrated with ^{22}Na and ^{228}Th γ -ray sources.

The time-of-flight spectrum was obtained by gating the RF start signal with triton events from the focal plane. Random events are observed with every beam burst, but the number of prompt coincidence events is typically three times larger. Reducing the beam current would improve this ratio. A small peak delayed by 30 ns is from the γ flash coming back from the beam stop. It is worth noting that the chosen geometry did not require any shielding. Coincidence events shown in Fig. 1 below represent true coincidences obtained as difference between prompt and random events.

Due to the short distance between detector and target, time of flight can be used to select neutrons for the energy interval 0.2 to 10 MeV, but it cannot be used for precise neutron energy determination. However, the neutron-deuteron interaction in the deuterated NE230 scintillator leads to a characteristic response function which will make it possible to unfold the pulse height spectrum and deduce the neutron spectrum with moderate resolution. Preliminary estimates for the neutron detection efficiency are 10 - 15%. The total detection efficiency for neutrons from an evaporation spectrum is estimated for the chosen geometry to be several times 10^{-3} per detector.

Pulse-shape discrimination was employed to separate neutrons and γ -rays detected in the scintillator. This was done using hardware discrimination.

Figure 2 (top part) displays the triton energy spectrum up to $E_x = 50\text{ MeV}$ obtained in two overlapping momentum bites for $^{120}\text{Sn}(^3\text{He},t)$ over the angular range from -1° to $+3^\circ$. The spectrum is dominated by two intense sharp peaks from singly-ionized $^3\text{He}^+$ and from the transition to the IAS in ^{120}Sb at $E_x = 10.20\text{ MeV}$. The IAS cross section at 0° is estimated to be about 8 mb/sr. Also seen are weak transitions to the 1^+ ground state in ^{120}Sb and other low-excited states, as well as broad resonances superimposed on a continuum. The broad structures near 12 MeV and 21 MeV can be identified with the Gamow-Teller resonance and the charge-exchange E1 resonance ($T_<$ component of M1 and E1) observed previously³ in low-energy (p,n). The E1 resonance observed in the (p,n) work (45 MeV/u) is assumed³ to be a non-spin flip resonance, but spin flip may contribute at our slightly higher bombarding energies (65 MeV/u).

Ray-tracing was used to separate the observed spectrum into the two angular ranges centered at 0° and 2° , respectively. These spectra are included in Fig. 2. Singly-ionized $^3\text{He}^+$ and $L=0$ transitions are strongly favored at 0° , whereas $L=1$ transitions are about equally strong at the two angles. The 2° spectrum, therefore, favors $L=1$ with a reduced contribution from $L=0$ transitions. The difference spectrum $0^\circ - 2^\circ$ (bottom part) shows the strong selectivity to $L=0$ transitions including the IAS and GT resonances. A broad structure centered near $E_x = 30\text{ MeV}$ is seen in the difference spectrum. Its excitation energy, width, and cross section are approximately compatible with calculated properties⁴

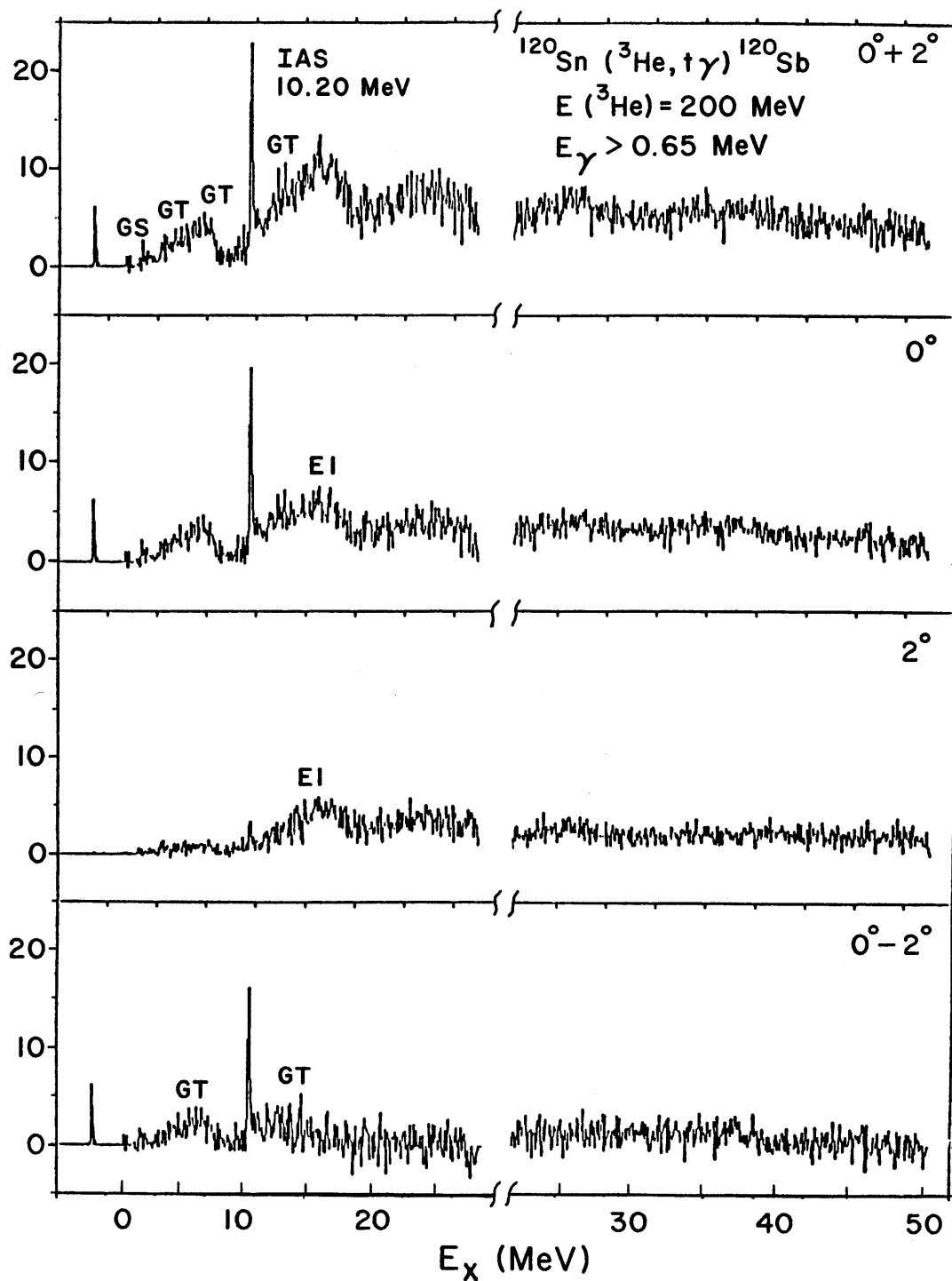


Figure. 1. Triton energy spectrum from $^{120}\text{Sn}(^3\text{He}, t)$ at $E(^3\text{He}) = 200 \text{ MeV}$ measured with the K600 spectrometer in coincidence (true = prompt - random) with γ -rays following neutron decay. The four spectra are again from two overlapping exposures, and they represent the same angular ranges as in Fig. 2.

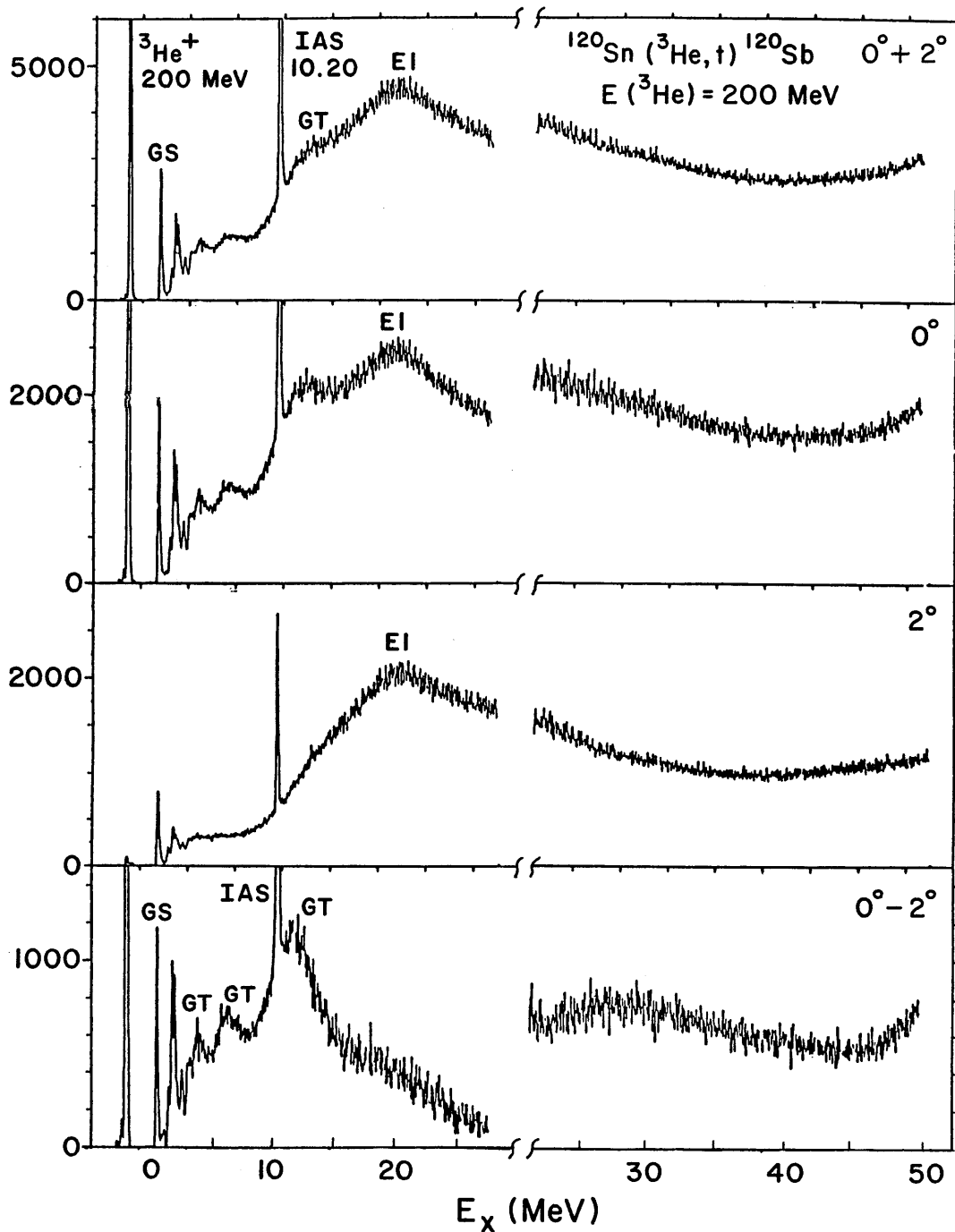


Figure 2. Triton energy spectrum from $^{120}\text{Sn}(^3\text{He},t)^{120}\text{Sb}$ at $E(^3\text{He}) = 200$ MeV measured with the K600 spectrometer for the angular range $-1^\circ \leq \Theta_t \leq +3^\circ$, and separately centered at 0° and 2° . The spectrum at the bottom displays the difference for $0^\circ - 2^\circ$. The spectra were obtained with two overlapping exposures. The vertical scales are expanded, and the small angle peaks from singly ionized $^3\text{He}^+$ and the isobaric analog state are cut off. The separation of the observed spectra into 0° and 2° components is still imperfect in our preliminary analysis.

of the isovector giant monopole resonance (IVGMR). However, confirmation through coincidence data is still required. An increase in the forward-angle spectrum above $E_x = 47$ MeV is not understood. It may be another resonance or possible pick-up, break-up.

Figure 1 displays one of the corresponding triton energy spectra observed in coincidence with decay particles. The spectra of Fig. 1 were obtained in coincidence with γ -rays following primary and sequential neutron emission. Similar spectra obtained in coincidence with decay neutrons directly (not shown) display the IAS and GT resonances. However, the statistics in our preliminary analysis are poor because of the (software) energy threshold for neutrons which is typically more than 5 times higher than the corresponding γ -ray threshold setting. The observed IAS intensity is compatible with the expected⁵ branching ratio of close to 100% for the neutron decay of the IAS (spreading width). Neutron decay from the IAS in medium-heavy and heavy nuclei following charge exchange has apparently not been observed before. Fig. 1 shows that the IAS is again very weak in the 2° spectrum in agreement with the expected angular behavior. The coincidence spectrum also displays forward peaked giant resonances in approximate agreement with the observed $T_{<}$ components of the M1 and E1 giant resonances in the target nucleus.³ The resonances may display fine structure, and the possible presence of an E1 resonance near $E_x = 16$ MeV seems to be indicated. Compared to Fig. 2, Fig. 1 shows giant resonances very clearly despite the much lower statistics, presumably because of a suppression of the underlying background from the nuclear continuum including breakup/pickup reactions.

Results very similar to those of Figs. 1 and 2 were also obtained for the reaction $^{117}\text{Sn}(^3\text{He},t)$ up to $E_x = 25$ MeV. The branching ratio for neutron decay from the IAS in ^{117}Sb appears to be less than 100% in agreement with earlier results which suggest competition with proton decay.⁵ Compared to ^{120}Sb , the GT resonance in ^{117}Sb appears to be fragmented even more.

Despite the limited statistics, the reported results clearly demonstrate the power of the experimental techniques in suppressing the nuclear continuum and in detecting and studying especially the $L=0$ and $L=1$ charge-exchange giant resonances and their decay modes, both from non-spin flip and spin flip transitions. Measurements with greatly increased neutron detection efficiency (more detectors) and better statistics are planned.

This work was supported in part by grants from NSF, FOM (NL), and NATO (travel grant).

1. C.D. Goodman, C.A. Goulding, M.B. Greenfield, J. Rapaport, D.E. Bainum, C.C. Foster, W.G. Love and F. Petrovich, *Phys. Rev. Lett.* **44**, 1755 (1980); G.F. Bertsch and H. Esbensen, *Rep. Prog. Phys.* **50**, 607 (1987).
2. J. Jänecke et al., *Bull. Am. Phys. Soc.* **33**, 1595 (1988); *ibid.* **34**, 1232 (1989); *ibid.* IUCF Newsletter 42, April 1988, p. 21; *ibid.* IUCF Scientific and Technical Report, January 1987 - April 1988, p. 48; *ibid.* IUCF Newsletter 44, 31 March 1989, p. 30.
3. W.A. Sterrenburg, S.M. Austin, R.P. DeVito and A. Galonsky, *Phys. Rev. Lett.* **45**, 1839 (1980).
4. N. Auerbach and A. Klein, *Nucl. Phys.* **A395**, 77 (1983).
5. F.D. Becchetti, W.S. Gray, J. Jänecke, E.R. Sugarbaker and R.S. Tickle, *Nucl. Phys.* **A271**, 77 (1976).